

Original article

Myocardial autophagy activation and suppressed survival signaling is associated with insulin resistance in fructose-fed mice

Kimberley M. Mellor^a, James R. Bell^a, Morag J. Young^c, Rebecca H. Ritchie^{b,d,1}, Lea M.D. Delbridge^{a,*,1}^a Department of Physiology, University of Melbourne, Melbourne, VIC, Australia^b Department of Pharmacology, University of Melbourne, Melbourne, VIC, Australia^c Prince Henry's Institute of Medical Research, Clayton, VIC, Australia^d Heart Failure Pharmacology, Baker IDI Heart and Diabetes Institute, Melbourne, VIC, Australia

ARTICLE INFO

Article history:

Received 8 February 2011

Accepted 1 March 2011

Available online 6 March 2011

Keywords:

Dietary fructose

Myocardial autophagy

ROS

Signaling

Insulin resistance

ABSTRACT

Fructose intake is linked with the increasing prevalence of insulin resistance and there is now evidence for a specific insulin-resistant cardiomyopathy. The aim of this study was to determine the cardiac-specific myocardial remodeling effects of high fructose dietary intake. Given the links between insulin signaling, reactive oxygen species generation and autophagy induction, we hypothesized that autophagy contributes to pathologic remodeling in the insulin-resistant heart, and in particular may be a feature of high fructose diet-induced cardiac phenotype. Male C57Bl/6 mice were fed a high fructose (60%) diet or nutrient-matched control diet for 12 weeks. Systemic and myocardial insulin-resistant status was characterized. Superoxide production (lucigenin) and cellular growth and death signaling pathways were examined in myocardial tissue. Myocardial structural remodeling was evaluated by measurement of heart weight indices and histological analysis of collagen deposition (picrosirius red). Fructose-fed mice exhibited hyperglycemia and glucose intolerance, but plasma insulin and blood pressure were unchanged. High fructose intake suppressed the myocardial Akt cell survival signaling coincident with increased cardiac superoxide generation (21% increase, $p < 0.05$). Fructose feeding induced elevated autophagy (LC3B-II: LC3B-I ratio: 46% increase, $p < 0.05$) but not apoptosis signaling (unchanged Bax-1:Bcl-2 ratio). Despite a 28% increase in interstitial fibrosis, no difference in heart weight was observed in fructose-fed mice. We provide the first evidence that myocardial autophagy activation is associated with systemic insulin resistance, and that high level fructose intake inflicts direct cardiac damage. Upregulated autophagy is associated with elevated cardiac superoxide production, suppressed cell survival signaling and fibrotic infiltration in fructose-fed mice. The novel finding that autophagy contributes to cardiac pathology in insulin resistance identifies a new therapeutic target for diabetic cardiomyopathy.

© 2011 Elsevier Ltd. All rights reserved.

1. Introduction

Large population studies have recently demonstrated that high dietary sugar is associated with increased risk for type 2 diabetes and cardiovascular disease independent of body mass index [1–4]. There is increasing evidence that fructose intake in particular, is linked to insulin resistance [2], and animal models confirm that a high fructose diet disturbs metabolic homeostasis and reduces insulin sensitivity [5,6]. Cardiovascular disease and type 2 diabetes are frequently coincident and evidence for a specific insulin-resistant cardiomyopathy is emerging [7–9]. In type 2 diabetic experimental genetic models (i.e. *ob/ob* and *db/db* mice, and Zucker fatty rats) cardiac hypertrophy has been observed [10], occurring in association with

hypertension and severe obesity. The direct cardiomyopathic consequences of chronic high fructose intake are not yet mechanistically well defined, but a number of experimental studies have demonstrated that ventricular dysfunction is associated with elevated dietary fructose [11–13].

The myocardium may be especially vulnerable to the deleterious influence of high fructose intake, given that it is both an insulin-sensitive and glycolysis-dependent tissue. Although fatty acid oxidation constitutes the majority (60–90%) of cardiomyocyte ATP production, there is evidence that specific excitation–contraction coupling processes may be particularly reliant on glycolytically-derived ATP supply [14]. Fructose bypasses the phosphofructokinase rate-limiting step of glycolysis, and high fructose availability creates the potential for relatively unrestrained production of glycolytic end products and cellular metabolic dysregulation [15]. In addition, fructose-induced insulin resistance may manifest as alterations in cardiac signaling through the insulin-responsive phosphoinositide-3-kinase (PI3K)/Akt pathway. This pathway is known to regulate

* Corresponding author at: Department of Physiology, University of Melbourne, Parkville, Victoria 3010, Australia. Tel.: +61 3 83445853; fax: +61 3 83445818.

E-mail address: lmd@unimelb.edu.au (L.M.D. Delbridge).

¹ Co-senior authors.

glucose uptake, cardiac growth, and cell survival [16]. Although fructose-induced signaling abnormalities in skeletal muscle have been described [17], these effects have not been identified in the myocardium.

The involvement of autophagy in mediating cell survival is increasingly recognized. Autophagy is an intracellular degradation process activated during stress conditions to support substrate regeneration and is characterized by vacuolar destruction of macromolecules and organelles [18]. Excessive autophagy leads to a distinctive non-apoptotic programmed cell death in pathological myocardial remodeling [19]. Reactive oxygen species (ROS) have been shown to induce autophagy in various tissue types [20] and in the heart autophagy is activated post-ischemia in association with ROS upregulation [21]. ROS play an early role in the development of tissue insulin resistance [8,9] and even short-term fructose feeding increases myocardial ROS production [22]. There is some evidence that downstream components of the PI3K/Akt insulin-responsive signaling pathway may be the target of exogenous inducers of autophagy [23].

Given the regulatory associations between Akt, ROS and autophagy, we hypothesized that autophagy contributes to pathologic remodeling in the insulin-resistant heart, and in particular may be a feature of high fructose diet-induced cardiac phenotype. We now identify a specific fructose-induced cardiac remodeling pathology, occurring in the absence of hypertension and obesity. This study provides the first evidence that insulin resistance is associated with myocardial autophagy activation coincident with ROS upregulation and suppression of the PI3K/Akt survival signaling pathway.

2. Materials and methods

2.1. Dietary treatments and in vivo measurements

Male C57Bl/6 mice were housed in temperature-controlled conditions in a 12 h light/dark cycle, and were cared for in accordance with the Australian Code of Practice for the Care and Use of Animals for Scientific Purposes, and procedures approved by the Animal Ethics Committee of the University of Melbourne. The investigation conforms with the *Guide for the Care and Use of Laboratory Animals* published by the US National Institutes of Health (NIH Publication No. 85-23, revised 1996). At the commencement of the dietary treatment period, mice aged 4–5 weeks were allocated to either a control (54% starch, 10% sucrose, 7% total fat, 19.4% protein) or high fructose (60% fructose, 3.6% starch, 7% total fat, 19.4% protein) diet, as previously detailed [22]. The diets were based on the American Institute of Nutrition standard rodent growth diet [24], were of equal digestible energy and were micro- and macro-nutrient matched (AIN93G, SF03-018; Specialty Feeds, WA, Australia). In the final week of treatment, blood pressure was measured in a subgroup of mice on 3 consecutive days using tail cuff plethysmography [25], as previously described [22]. A glucose tolerance test was performed on another subgroup of mice (fasted 6 h) during week 12 of the dietary manipulation. Blood samples (~10 µl) were collected by tail prick for determination of blood glucose using a glucometer (ACCU-CHEK® Advantage, Roche, Mannheim, Germany) prior to and following injection with 1.5 mg/g glucose solution i.p. (15, 30, 60 and 90 minutes post-injection).

2.2. Tissue and plasma collection

At the completion of the 12 week feeding period (age 16 weeks), all mice were fasted for 3–4 hours, heparinized (1000 IU, i.p.) and anesthetized by sodium pentobarbitone (60 mg/kg i.p.). Cohorts of mice were allocated to measurements of ROS production, molecular biology (Westerns, real time RT-PCR), histology or myocyte isolation. Trunk blood was collected for measurement of blood glucose and plasma insulin (Rat Insulin RIA kit; LINCO Research, MO, USA)

concentrations. Cardiac weight index was determined as heart weight (mg): tibia length (mm). Ventricles were sectioned into equal portions comprising both right and left ventricle for immediate assessment of myocardial superoxide production or snap-frozen for later molecular analysis.

2.3. Detection of myocardial superoxide production

NADPH-driven superoxide production, an estimate of NADPH oxidase activity, was measured in freshly-dissected ventricular tissue fragments (6 fragments per heart, 1–2 mm) using lucigenin-enhanced chemiluminescence as previously described [22]. Superoxide production was expressed as counts/s/mg dry tissue.

2.4. Western blot analysis of myocardial protein expression

Frozen cardiac tissues were homogenized in Tris–HCl 100 mM, EGTA 5 mM, EDTA 5 mM (Sigma Aldrich, MO, USA) buffer containing protease and phosphatase inhibitors (Roche, Basel, Switzerland). Crude homogenate samples were analyzed for protein expression of S6, p38 mitogen activated protein kinase (MAPK), light chain 3 (LC3B), extracellular signal regulated kinase (ERK1/2), Glut4 and p62 (SQSTM1). Aliquots of crude homogenate samples were centrifuged at 17,500g for 10 minutes at 4 °C and the supernatants containing cytosolic proteins were collected for analysis of Akt and Beclin-1. An autophagy positive control sample (36 h fasted mouse heart) was used to determine optimal conditions for all autophagy markers. Sample protein concentration was determined by a modified Lowry assay [26]. Protein expression was determined by SDS–PAGE and Western blotting. Phospho-S6 (Ser235/236), S6, phospho-p38MAPK (Thr180/Tyr182), p38MAPK, phospho-ERK1/2 (Thr202/Tyr204), ERK1/2, phospho-Akt (Ser473), Akt, Beclin-1, LC3B antibodies were obtained from Cell Signaling Technology, Inc. (MA, USA). The p62 (SQSTM1 (D-3)) antibody was obtained from Santa Cruz Biotechnology Inc. (CA, USA) and the Glut4 antibody was obtained from Abcam (Cambridge, UK). Replicate samples were utilized for Western blotting when necessary to reduce variability. Membranes were incubated with anti-rabbit HRP-conjugated secondary antibody (GE Healthcare UK Ltd, Buckinghamshire, UK). The ECL Plus (Amersham™, GE Healthcare UK Ltd, Buckinghamshire, UK) chemiluminescent signal was imaged and analyzed using Quantity One software (Biorad, CA, USA).

2.5. Real-time reverse transcription–polymerase chain reaction (RT–PCR)

RNA was extracted from frozen cardiac tissues using the TRIzol® reagent in conjunction with the PureLink™ Micro-to-Midi Total RNA Purification kit (Invitrogen, CA, USA) and was reverse transcribed using SuperScript™ III First-Strand Synthesis System (Invitrogen, CA, USA). Real-time PCR was used to determine the relative gene expression levels of the cardiac pro-hypertrophic gene (brain natriuretic peptide, BNP), mitochondrial antioxidant (thioredoxin 2, Thx2), pro- and anti-apoptotic genes (Bcl-2-associated protein, Bax, and Bcl-2), and the housekeeper gene (18S) in ventricular tissue. Primer sequences for each gene were as follows: BNP: 5'-CAGTCTCCAGAGCAATTCAAGATG-3' and 5'-CCATTTCCTCCGACTTTTCTCTTA-3'; Thx2: 5'-CAGCCTCTGGCA-CATTTCCT-3' and 5'-GTTCGGCTTCTGGTTCTTT-3'; Bax: 5'-GAGCTG-CAGAGGATGATTGCT-3' and 5'-GCGGCCCCAGTTGAAGT-3'; Bcl2: 5'-TGGGATGCCTTTGTGGAAT-3' and 5'-AGACAGCCAGGAGAAAT-CAAACA-3'; Glut4: 5'-CATGGCTGTCGCTGGTTTC-3' and 5'-AGCATCCG-CAACATACTGGAA-3' and 18S: 5'-TCGAGGCCCTGTAATTGGAA-3' and 5'-CCCTCCAATGGATCCTCGTT-3'. The comparative $\Delta\Delta C_t$ method was utilized to analyze the genes of interest as described [22,27].

2.6. Cardiomyocyte isolation and dimension measurements

Ventricular cardiomyocytes were isolated from a cohort of fructose- and control-fed mice, as described [28], using enzymatic digestion with Type II Collagenase (0.66 mg/ml, 295 U/mg, Worthington Biochemical Corporation, NJ, USA), and Trypsin (33 µg/ml; Sigma-Aldrich, MO, USA). Cardiomyocytes were resuspended in normal potassium, Ca²⁺-free HEPES-buffered Krebs and maximal cell width and length measured under 400× magnification (Nikon, Japan) using a calibrated graticule eye-piece ($n = 50$ cells/heart). Myocyte volume was calculated from individual myocyte area based on the previously demonstrated correlation between these parameters [29,30].

2.7. Histological analysis of myocardial collagen content

Hearts were excised from a separate cohort of mice fed the high fructose or control diet, and fixed in 10% formalin for histological analysis using picosirius red as previously described [31]. Images were captured with brightfield microscopy using the Olympus DP Controller software (V2.3.1.231, Olympus, Japan) with 18–20 images per section, from 3 sections per heart. Image analysis was performed using Image Pro Plus (V4.5.1, Media Cybernetics, MD, USA) in a 'blinded' manner. Briefly, images were converted to grey scale (255 pixel range), a pixel intensity histogram was assessed to determine the non-bias threshold point of collagen staining. A binary map of collagen deposition was generated, from which collagen density (represented in 'black') was calculated and expressed relative to the total number of pixels in the area of interest.

2.8. Statistical analyses

Data are expressed as mean (\pm standard error) and were analyzed with Student's unpaired *t*-test with the exception of glucose tolerance data, which was analyzed by 1-way ANOVA, repeated measures test. A *p*-value <0.05 was considered statistically significant.

3. Results

3.1. Fructose feeding induces metabolic perturbations

Mice were matched for body weight at the commencement of the feeding period. After a 12 week treatment, the mean body weight in the fructose-fed group was 7% lower than the control-fed group (Table 1). As shown in Table 1, fasted blood glucose concentrations were 26% higher in fructose-fed mice relative to controls ($p < 0.05$). Plasma insulin levels and blood pressure were comparable between the two groups (Table 1). A glucose tolerance test (GTT) was performed on fasted (6 h) mice. Fructose-fed mice exhibited a slower glucose disappearance rate following the 1.5 g/kg glucose load, indicative of systemic insulin resistance (Fig. 1A). This corresponded to a 14% increase in the area under the GTT curve in the fructose group relative to controls ($p < 0.05$, Fig. 1B). Thus, fructose-fed mice were hyperglycemic but not hyperinsulinemic under fasted conditions and exhibited early signs of insulin resistance.

Table 1
Systemic characteristics of control- and fructose-fed mice.

	Control	Fructose
Body weight (g)	25.7 \pm 0.5	24.0 \pm 0.2*
Blood glucose (mM)	11.7 \pm 0.9	14.8 \pm 0.8*
Plasma insulin (ng/ml)	0.93 \pm 0.11	0.82 \pm 0.08
Blood pressure (mm Hg)	98.6 \pm 3.2	94.6 \pm 5.6

Mice were fasted 3–4 h prior to glucose and insulin measurements. Data presented as mean \pm s.e.m. $n = 6$ –9 mice/group.

* $p < 0.05$.

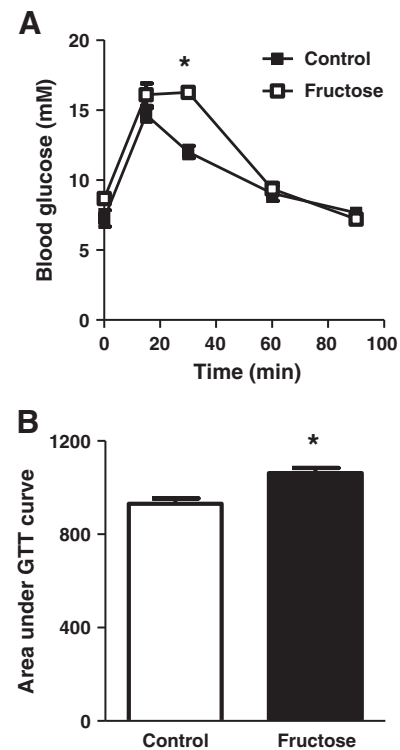


Fig. 1. Assessment of glucose tolerance in control- and fructose-fed mice (fasted 6 h). A. Glucose disappearance following 1.5 g/kg glucose load. Note—in some instances error bars are not discernable as they fall within symbol shapes. B. Area under the glucose tolerance curve. Data presented as mean \pm s.e.m. $n = 5$ –6. * $p < 0.05$.

3.2. Suppressed myocardial survival and trophic signaling induced by a high fructose diet

Given this evidence of systemic insulin resistance, we evaluated the influence of high fructose intake on myocardial signaling via the insulin-sensitive PI3K/Akt axis. After 12 weeks of dietary treatment, phosphorylated (Ser473) to total Akt protein expression was down-regulated in fructose-fed mice relative to control-fed mice ($p < 0.05$). Consistent with reduced Akt activity, phosphorylated (Ser235/236) to total S6 was 57% lower in fructose-fed mice ($p < 0.05$, Fig. 2B). Gene and protein expression of basal total Glut4 was similar between groups. To further assess the effect of high fructose intake on trophic signaling, activation of selected MAPK pathway intermediates was examined. Fructose-fed mice exhibited significantly reduced phosphorylated (Thr180/Tyr182) to total p38-MAPK protein, indicative of downregulated growth signaling (Fig. 3A). No change in phosphorylated (Thr202/Tyr204) to total ERK1/2 was observed in response to high fructose (Fig. 3B).

3.3. Myocardial remodeling effects of a high fructose diet

To determine whether alterations in PI3K/Akt and p38MAPK signaling corresponded to cardiac morphological changes, we measured cardiac weight indices, hypertrophic gene expression and myocardial collagen deposition. The fructose dietary manipulation had no effect on heart weight or on heart weight normalized to tibia length (Fig. 4A and B). Similarly, ventricular weight did not differ between groups (data not shown). Despite no change in heart weight or isolated cardiomyocyte size (Table 2), gene expression of the cardiac growth marker, BNP, was dramatically reduced in fructose-fed mice relative to control-fed mice (58% decrease, $p < 0.05$). As depicted in Fig. 4D–F, fructose-fed mice exhibited a significant increase in total ventricular collagen deposition, with a 28% increase in interstitial cross-section area occupied by collagen compared with controls.

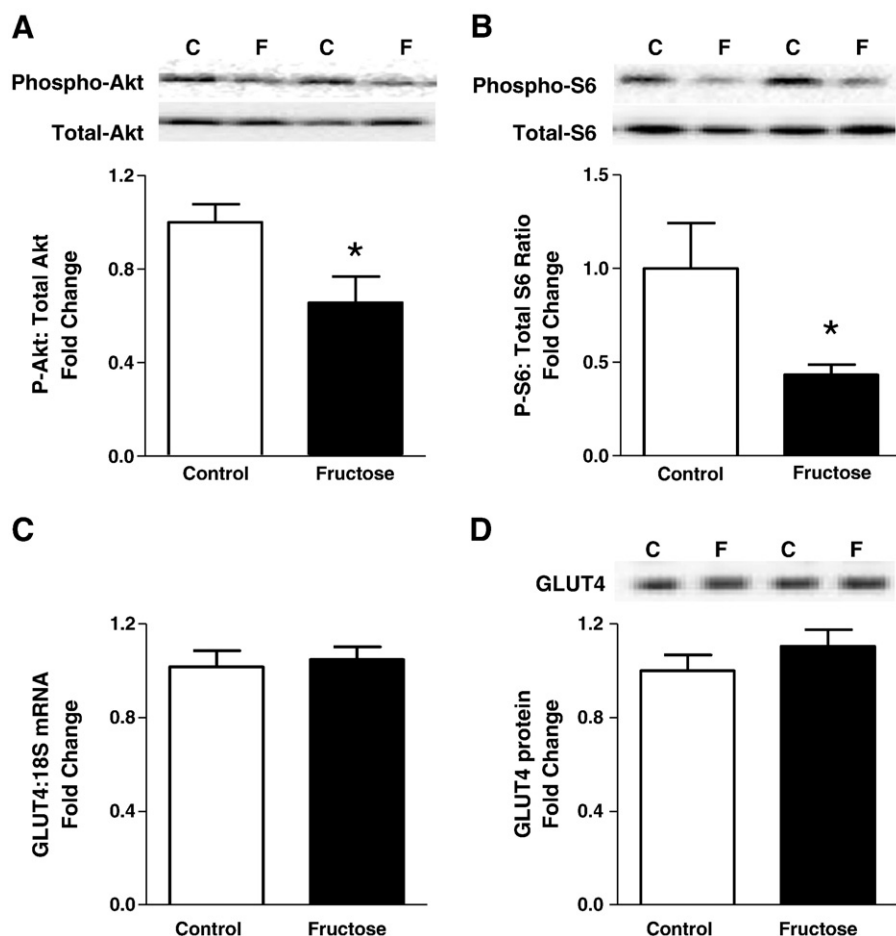


Fig. 2. Cardiac signaling effects of a high fructose diet. A. Protein expression of Phospho-Akt normalized to Total-Akt ($n = 5-6$). B. Protein expression of Phospho-S6 normalized to Total-S6 protein ($n = 9-10$). C. GLUT4 gene expression normalized to 18S in ventricular tissue ($n = 8-9$). D. Protein expression of GLUT4 ($n = 8-9$). Data presented as mean \pm s.e.m. * $p < 0.05$.

Collagen deposition is diffuse, consistent with distributed fibrotic infiltration and myocyte replacement. Estimation of myocyte number using myocardial mass (i.e. heart weight adjusted for collagen deposition) and myocyte size (i.e. estimated from myocyte volume data) was calculated. It is estimated that fructose treatment was associated with a 4% reduction in myocyte number (Table 2).

3.4. Fructose-induced myocardial ROS production

Given the evidence that ROS play a role in myocardial insulin resistance and remodeling [9,32], we examined myocardial superoxide production after 12 weeks of high fructose intake. As presented in Fig. 5A, high fructose intake for 12 weeks was associated with a

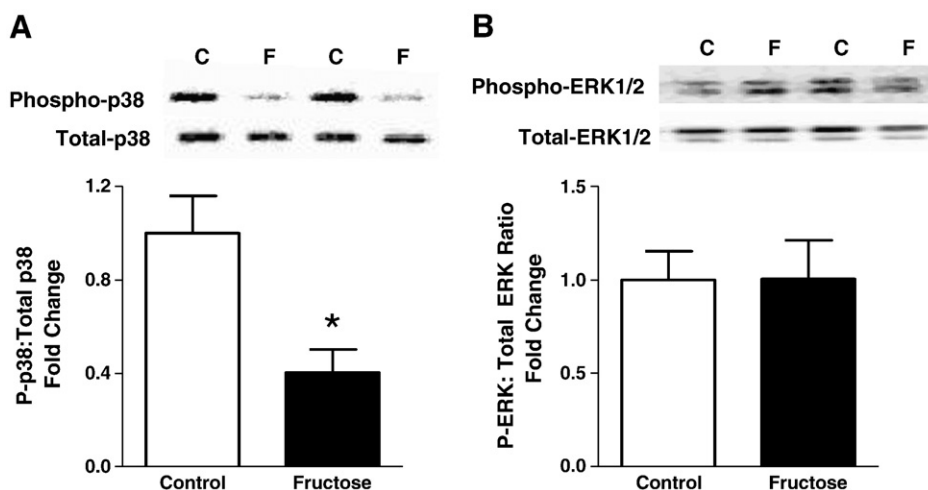


Fig. 3. Cardiac MAPK signaling effects of a high fructose diet. A. Protein expression of Phospho-p38MAPK normalized to Total-p38MAPK ($n = 9$). B. Protein expression of Phospho-ERK1/2 normalized to Total-ERK1/2 ($n = 10$). Data presented as mean \pm s.e.m. * $p < 0.05$.

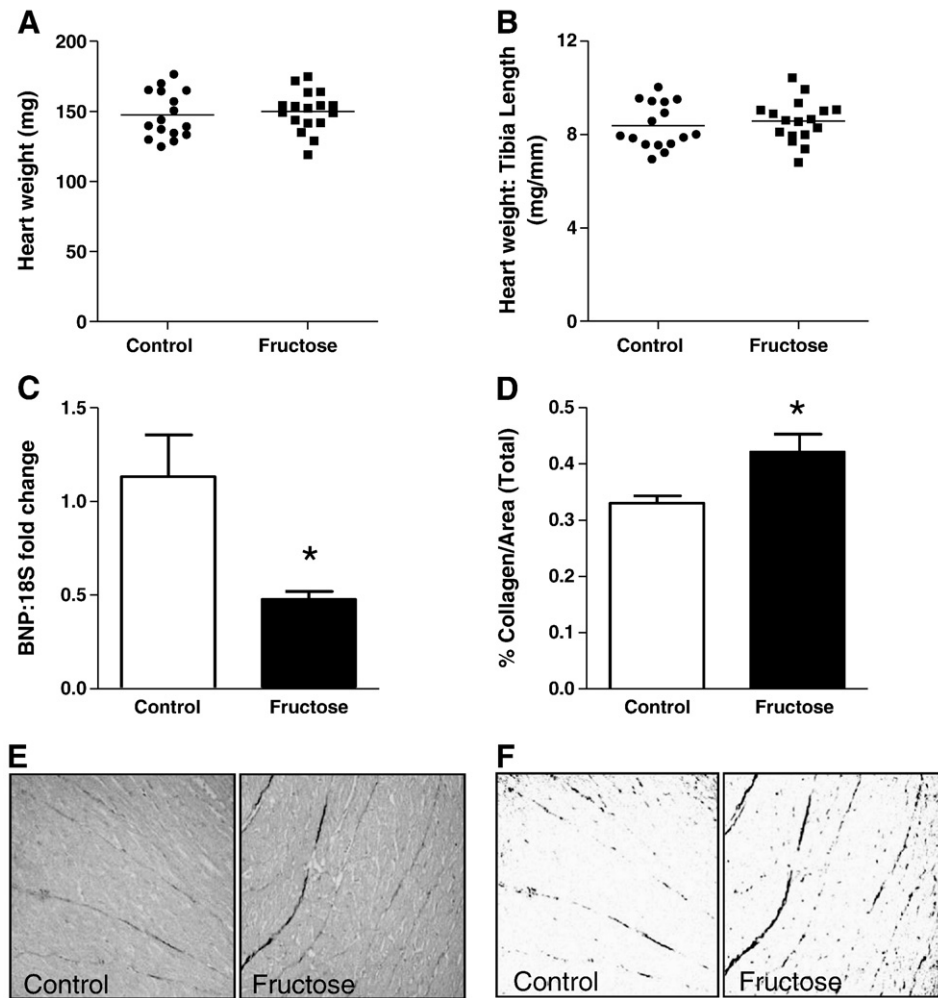


Fig. 4. Cardiac structural remodeling effects of a high fructose diet. A. Heart weights ($n = 16$ – 17). B. Heart weights normalized to tibia length ($n = 16$ – 17). C. BNP gene expression normalized to 18S in ventricular tissue ($n = 8$). D. Total collagen (as a % of image area) in picrosirius red stained sections of ventricular tissue ($n = 3$ sections/heart; $n = 6$ – 8 hearts). E. Representative grey scale images of picrosirius red stained ventricular sections from control- and fructose-fed mice. F. Binary maps derived from Fig. 4E, by image thresholding and segmentation. Collagen positive areas are set to 'black' for quantification. Data presented as mean \pm s.e.m. * $p < 0.05$.

significant elevation in ventricular NADPH-driven superoxide production (fructose 553 ± 28 counts/s/mg vs. control 456 ± 17 counts/s/mg, $p < 0.05$), indicative of increased NADPH oxidase activity. Gene expression of the cardiac mitochondrial antioxidant, Thioredoxin2, was comparable between the groups (Fig. 5B), suggesting elevated ROS production was not matched by an increased antioxidant defense.

3.5. Cardiomyocyte autophagy is activated in fructose-fed mice

Despite evidence of fibrosis, whole heart weights were not changed in fructose-fed mice. Potentiated myocyte loss through

programmed cell death (apoptosis, autophagy) was thus examined. LC3B-II is required for the formation of autophagosomes; LC3B-I resides in the cytosol and is the inactive form of LC3B. The ratio of active to inactive LC3B (i.e. LC3B-II:LC3B-I protein expression) was increased by 46% in the fructose-fed mice relative to controls ($p < 0.05$, Fig. 6A), indicative of increased autophagic activity. Consistent with the effect on LC3B, fructose-fed mice exhibited a trend ($p = 0.11$) for increased Beclin-1 protein expression (an activator of autophagy). Protein expression of the autophagic marker p62 (an adaptor protein involved in linking polyubiquitylated protein aggregates and the autophagic machinery) was similarly upregulated in the fructose-fed mouse hearts (Fig. 6C). Myocardial gene expression of apoptosis regulators, Bax-1 (pro-apoptotic) and Bcl-2 (anti-apoptotic) were evaluated (Fig. 7). Expression levels of these proteins were similarly reduced, Bax-1 by 32.6% ($p < 0.05$) and Bcl-2 by 29.7% ($p = 0.14$). With similar reductions, there was no net effect on the Bax-1/Bcl-2 ratio, suggesting no evidence of apoptosis activation.

4. Discussion

This study provides the first evidence that myocardial autophagic activation is associated with insulin resistance. In mice fed a high fructose diet for a period of 12 weeks, myocardial ROS production and fibrosis were upregulated, and signaling via the insulin-sensitive PI3K/Akt cell survival pathway was suppressed coincident with

Table 2

Dimensions of cardiomyocytes from control- and fructose-fed mice.

	Control	Fructose
Width (μm)	25.5 ± 0.3	27.2 ± 0.8
Length (μm)	138 ± 3	137 ± 5
Area (μm^2)	3530 ± 60	3740 ± 210
Volume (pL)	26.8 ± 0.5	28.4 ± 1.6
Estimated myocyte number	5,510,000	5,290,000

Cardiomyocyte volume calculated (pL) = $7.59 \times 10^{-3} \times \text{length } (\mu\text{m}) \times \text{width } (\mu\text{m})$ [29]. Estimated myocyte number = myocardial mass (g; heart weight adjusted for collagen deposition) / myocyte size (g; estimated from myocyte volume) and is a mean comparison for an 'average' heart in each group (all hearts, not an estimate per individual heart). Data presented as mean \pm s.e.m. ($n = 50$ cells/mouse; $n = 5$ mice/group).

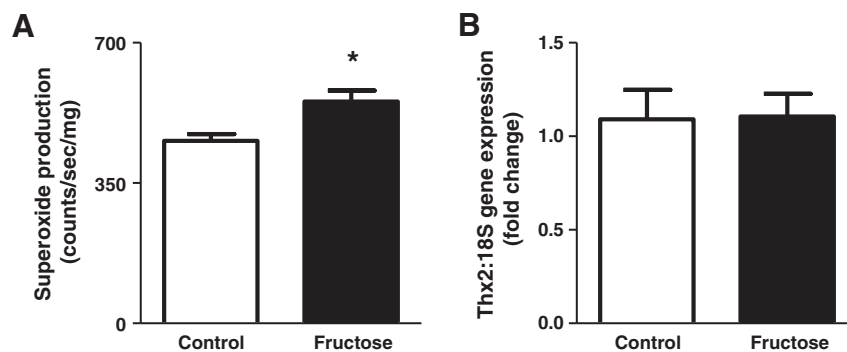


Fig. 5. Impact of fructose feeding on myocardial redox status. A. Myocardial NADPH-stimulated superoxide (O_2^-) production normalized to dry tissue weight ($n=10-11$). B. Thioredoxin2 gene expression normalized to 18S in ventricular tissue ($n=8-9$). Data presented as mean \pm s.e.m. * $p<0.05$.

increased levels of the autophagosomal activity markers, LC3B-II and p62. No cardiac hypertrophy was evident. On the basis of cell size analysis, an estimate of myocyte numbers suggests that fibrotic infiltration may occur in association with myocyte loss. As the systemic/peripheral insulin resistance was relatively modest in these fructose-fed mice and because there was an absence of other hemodynamic loading complications (no hypertension or obesity), the cardiac effects could be interpreted as direct rather than indirect actions on myocardial insulin signaling pathways.

4.1. Fructose feeding induces an insulin-resistant phenotype

It has been previously demonstrated that fructose feeding disturbs systemic metabolism and induces insulin resistance in rats [5,6]. In this study in mice, 12 weeks of fructose feeding induced glucose-intolerance, coincident with hyperglycemia. Plasma insulin levels were unchanged. Acutely, fructose is known to stimulate hepatic glycogen breakdown and gluconeogenesis [33]. The present finding demonstrates that in mice, chronic high fructose intake produces a maintained hyperglycemia, in a context where hyperinsulinemia may not be detected. In rats, high fructose intake induces hyperinsulinemia and hypertension [34–36]. Although direct study comparisons are problematic (due to unmatched diets, reviewed in Mellor et al. (2010) [37]), the few available murine fructose feeding studies indicate that the systemic effects of a high fructose diet in mice are more subtle than those in the rat [36,38]. The present study has demonstrated that a well-controlled high fructose dietary intervention does not alter blood pressure in mice, consistent with our previous findings involving shorter term feeding intervention [22]. Many rodent models of diabetic cardiomyopathy (*ob/ob* mice, *db/db* mice, high fat-fed rats/

mice, Zucker fatty rats) are complicated by the coincident obesity-and/or hypertension-induced loading effect on the heart [10]. The extent of obesity, hyperinsulinemia and hyperglycemia which may be evident in such models is considerably more severe than that generally observed in patients with type 2 diabetes.

In the absence of hypertension and obesity, we detected fructose-induced insulin resistance at the myocardial tissue level, with a 35% down-regulation in Akt phosphorylation. Reduced signaling through the insulin-stimulated PI3K/Akt pathway is a recognized feature of insulin resistance in skeletal muscle [39], which relies on activation of this signaling pathway to manage trafficking of Glut4 transporters to support glucose uptake on demand. In the heart, where the activity demand is continuous, reduction in basal state Akt signaling is indicative of a chronic response to sustained metabolic perturbation. In the present study, downregulated Akt signaling occurred in the absence of altered plasma insulin, suggestive of a role for intracellular modification of this pathway. Total Glut4 expression was unchanged by the high fructose diet; thus it is feasible that suppression of the Akt signaling pathway would result in reduced translocation of Glut4 to the plasma membrane. In agreement with our findings, Briat et al. (2007) reported that a high fructose diet suppressed glucose uptake in cardiac tissue, as measured by the tracer 6-deoxy-6-endo-D-glucose (6DIG) [40]. We have previously shown that genetic down-regulation of Glut4 expression in the heart has deleterious growth and functional effects [41,42]. In lean STZ-diabetic rats, myocardial Akt activity is reduced [43] although this response is not necessarily observed in hyperinsulinemic obese diabetic models [44,45]. In contrast to the current study, Chess et al. (2007) did not observe Akt down-regulation or hyperglycemia in fructose-fed mice [11]. The

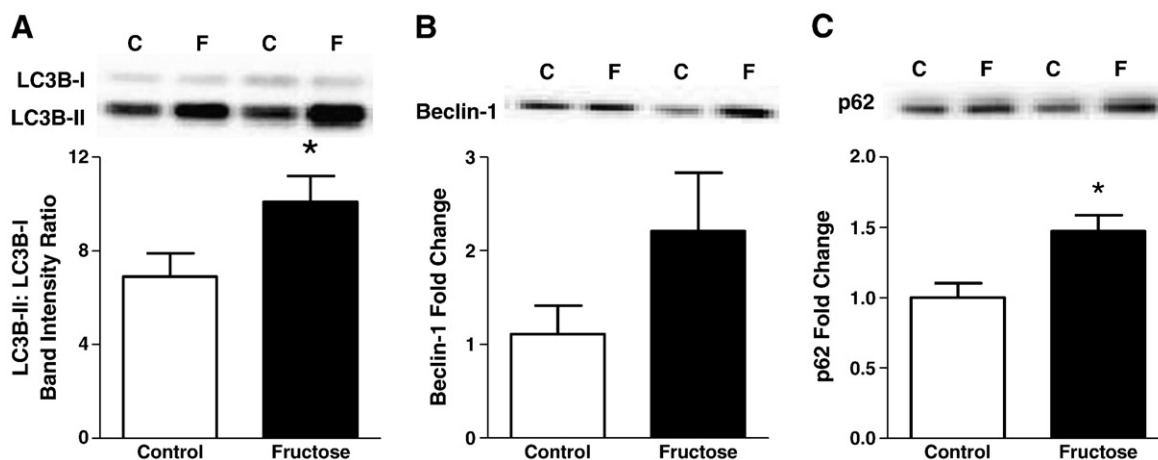


Fig. 6. Effect of a high fructose diet on myocardial autophagy. A. Ratio of active:inactive LC3B protein expression in ventricular tissue ($n=8$). B. Beclin-1 protein expression in ventricular tissue ($n=7-9$). C. p62 (SQSTM1) protein expression in ventricular tissue ($n=8$). Data presented as mean \pm s.e.m. * $p<0.05$.

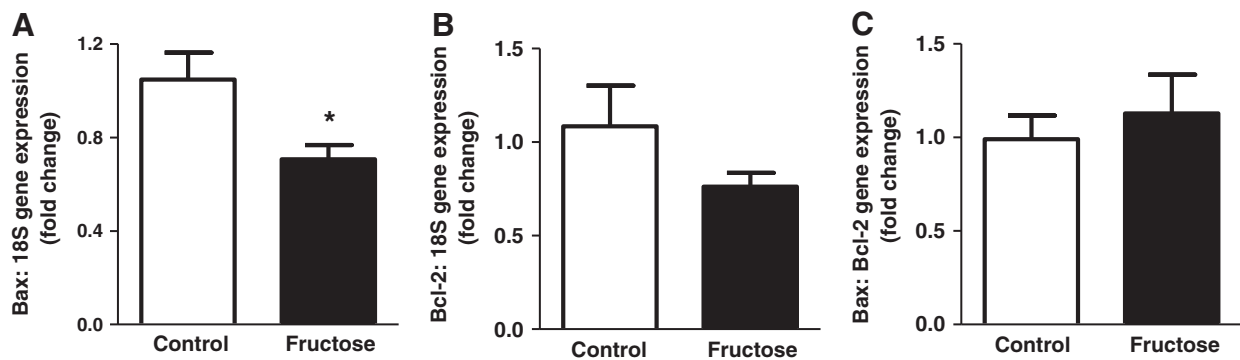


Fig. 7. Effect of a high fructose diet on myocardial apoptotic signaling. A. Pro-apoptotic Bax-1 expression normalized to 18S in ventricular tissue ($n=8$). B. Anti-apoptotic Bcl-2 expression normalized to 18S in ventricular tissue ($n=6-8$). C. Ratio of Bax:Bcl-2 expression in ventricular tissue ($n=6-8$). Data presented as mean \pm s.e.m. * $p<0.05$.

basis for these contrasting findings is unclear, but may be related to the higher levels of fat and soy specified in the diet used in the earlier study. In the present study, we identify evidence of both systemic and myocardial fructose-induced insulin resistance, which occur independent of systemic loading influences.

4.2. Activation of autophagy with suppressed cell survival signaling

This investigation is the first to provide evidence that an *in vivo* insulin-resistant phenotype is associated with activation of myocardial autophagy. Autophagy is a physiological process by which cells degrade and recycle macromolecules and organelles. Upregulated myocardial autophagy has been reported in starvation [46], heart failure [18] and ischemic heart disease [21]. Activation of this pathway can lead to programmed cell death and consequent myocyte loss in these settings, mediating the progression to heart failure [18,19,47]. A role for myocardial autophagy in the context of insulin-resistant or diabetic cardiac pathology has not been previously investigated. It is notable that autophagy in the heart was first demonstrated in neonates during the 'starvation' transition from placental to lactational nutrition [48]. Cardiomyocyte insulin resistance could be perceived as a cellular 'starvation' phenotype—a situation where glucose uptake is impaired through PI3K/Akt down-regulation and glucose availability is significantly limited. Our finding that Akt phosphorylation is down-regulated coincident with elevated LC3B-II and p62 levels indicates increased autophagosome formation. These findings provide 'static' evidence of increased autophagic activity. A detailed evaluation of autophagic flux in the setting of suppressed insulin-dependent Akt signaling is now required, to more fully describe altered autophagosome handling. The possibility that autophagy induction is also influenced by diurnal/fasting modulation should be considered.

In this investigation, 12 week fructose feeding was associated with an increase in NADPH-driven myocardial ROS production, detected using a lucigenin assay. This assay detects superoxide from a variety of sources including mitochondrially- and cytosolically-derived ROS [49]. Cardiac insulin resistance has been shown to induce a substrate preference switch from glucose to fatty acids [7]. Upregulated lipid metabolism, previously reported in fructose-fed rats [50], has the potential to increase ROS production. Evidence of elevated peroxisomal ROS generation associated with extra-mitochondrial processing of long chain fatty acids has been reported in a genetic model of myocardial insulin resistance [51]. Plasma fructose concentrations increase in response to a high fructose diet [52,53]. In non-cardiac tissues it has been demonstrated that fructose metabolism is relatively less regulated than glucose, by-passing the phosphofructokinase rate-limiting enzyme and leading to elevated lactate and acetyl CoA production [54]. This phenomenon is yet to be directly confirmed in cardiac tissues, but it may be speculated that increased acetyl CoA

metabolism would be linked with ROS generation. ROS-induced dephosphorylation of Akt at Serine473 has been reported [55]. Indeed, in the present study we show that reduced Akt phosphorylation at this ROS-target site is associated with elevated myocardial superoxide generation in fructose-fed mice. Characterization of the precise sources of superoxide production in fructose-fed mouse hearts would be informative. A mechanistic link between ROS production and autophagy induction has been demonstrated in cardiac cell lines [56,57] and may be the basis for the fructose-induced myocardial autophagy observed in the present study. New *in vitro* studies are warranted.

Beyond a role in mediating insulin-stimulated glucose uptake, the PI3K/Akt pathway has been implicated as a mediator of cell survival [16]. Activation of mTOR, a downstream component of the Akt pathway, has been shown to inhibit autophagy [58]. An involvement of mTOR in the context of high fructose intake is consistent with observations that the autophagocytic morphology of pancreatic beta islet cells in diabetes is partially recovered through treatment with metformin, an adenosine monophosphate-activated protein kinase (AMPK) activator which modulates mTOR [23]. Thus, the suppressed Akt signaling observed in the present study may relieve autophagic inhibition and contribute to myocyte loss. Our finding that Bcl-2 expression tended to be diminished by fructose feeding may also be relevant. In addition to involvement in apoptosis signaling, this protein protects against autophagy, through suppression of autophagy initiation via Beclin-1 [59]. Autophagy-induced programmed cell death is distinct from apoptosis [19] and this mode of cell death may be a key cellular response to fructose-induced insulin resistance stress. Although the present findings do not provide evidence of an increase in apoptosis signaling occurring in parallel with upregulated autophagy, further quantitative investigation comparing the relative contribution of type 1 and type 2 programmed cell death processes to myocyte attrition in the insulin-resistant myocardium is required.

4.3. Myocardial fibrosis and myocyte loss

The present study has demonstrated that despite increased interstitial collagen deposition, whole heart weight was unchanged. Previous studies have reported cardiac hypertrophy in fructose-fed rats—but in those studies cardiac growth was coincident with hypertension [60,61]. We have now demonstrated that, in the absence of systemic loading, heart size is not increased. Furthermore, the molecular signaling profile is not consistent with a pro-hypertrophic response. The cardiac growth marker, BNP, is actually reduced, as is p38-MAPK phosphorylation in fructose-fed mouse hearts (Fig. 4C). Thus, in the absence of loading, we could find no evidence of cardiac hypertrophy or cardiomyocyte enlargement in fructose-fed mice. Thus we suggest that the increased extracellular matrix volume is offset by myocyte loss, rendering net heart weight unchanged in

fructose-fed mice. Indeed, based on our myocyte volume data and the estimate of tissue volume occupied by fibrosis, we calculate that there has been a 4% reduction in cardiomyocyte number during 12 week fructose feeding. This relatively small loss over 12 weeks could be expected to have marked cumulative functional impact with ongoing extended dietary exposure. Indeed, Chang et al. (2007) reported cardiac dysfunction in *ex vivo* hearts in rats given 10% fructose drinking water [13]. Evaluation of functional outcomes at the cellular level are now required to assess the functional impact of autophagy induction with dietary fructose.

In conclusion, this investigation provides the first evidence that insulin resistance is associated with myocardial autophagy activation, accompanied by suppressed cell survival signaling and upregulated ROS production in fructose-fed mice. The novel finding that autophagy contributes to cardiac pathology in insulin resistance identifies a new therapeutic target for diabetic cardiomyopathy. The extent to which other models of insulin resistance and diabetes induce cardiac autophagy activation remains to be determined. Our work establishes that high fructose intake induces a cardiopathology that is not secondary to altered systemic loading conditions. Additional mechanistic work is now required to further characterize the link between altered insulin signaling and autophagy regulation in the heart and to demonstrate the direct causal role of modulated downstream PI3K signaling in autophagy induction.

Conflict of interest

There is none to declare.

Acknowledgments

This work was supported by the Diabetes Australia Research Trust, the National Heart Foundation of Australia, and the National Health and Medical Research Council of Australia (Senior Research Fellowship to R.H.R.).

References

- [1] Johnson RK, Appel LJ, Brands M, Howard BV, Lefevre M, Lustig RH, et al. Dietary sugars intake and cardiovascular health: A scientific statement from the American Heart Association. *Circulation* 2009;120(11):1011–20.
- [2] Stanhope KL, Schwarz JM, Keim NL, Griffen SC, Bremer AA, Graham JL, et al. Consuming fructose-sweetened, not glucose-sweetened, beverages increases visceral adiposity and lipids and decreases insulin sensitivity in overweight/obese humans. *J Clin Invest* 2009;119(5):1322–34.
- [3] Malik VS, Popkin BM, Bray GA, Despres JP, Hu FB. Sugar-sweetened beverages, obesity, type 2 diabetes mellitus, and cardiovascular disease risk. *Circulation* 2010;121(11):1356–64.
- [4] Dhingra R, Sullivan L, Jacques PF, Wang TJ, Fox CS, Meigs JB, et al. Soft drink consumption and risk of developing cardiometabolic risk factors and the metabolic syndrome in middle-aged adults in the community. *Circulation* 2007;116(5):480–8.
- [5] Lee MK, Miles PD, Khourshed M, Gao KM, Moossa AR, Olefsky JM. Metabolic effects of troglitazone on fructose-induced insulin resistance in the rat. *Diabetes* 1994;43(12):1435–9.
- [6] Basciano H, Federico L, Adeli K. Fructose, insulin resistance, and metabolic dyslipidemia. *Nutr Metab (Lond)* 2005;2(1):5.
- [7] Witteles RM, Fowler MB. Insulin-resistant cardiomyopathy clinical evidence, mechanisms, and treatment options. *J Am Coll Cardiol* 2008;51(2):93–102.
- [8] Ritchie RH. Evidence for a causal role of oxidative stress in the myocardial complications of insulin resistance. *Heart Lung Circ* 2009;18(1):11–8.
- [9] Mellor KM, Ritchie RH, Delbridge LM. Reactive oxygen species and insulin-resistant cardiomyopathy. *Clin Exp Pharmacol Physiol* 2010;37(2):222–8.
- [10] Bugger H, Abel ED. Rodent models of diabetic cardiomyopathy. *Dis Model Mech* 2009;2(9–10):454–66.
- [11] Chess DJ, Lei B, Hoit BD, Azimzadeh AM, Stanley WC. Deleterious effects of sugar and protective effects of starch on cardiac remodeling, contractile dysfunction, and mortality in response to pressure overload. *Am J Physiol Heart Circ Physiol* 2007;293(3):H1853–60.
- [12] Chess DJ, Xu W, Khairallah R, O'Shea KM, Kop WJ, Azimzadeh AM, et al. The antioxidant tempol attenuates pressure overload-induced cardiac hypertrophy and contractile dysfunction in mice fed a high fructose diet. *Am J Physiol Heart Circ Physiol* 2008;295(6):H2223–30.
- [13] Chang KC, Liang JT, Tseng CD, Wu ET, Hsu KL, Wu MS, et al. Aminoguanidine prevents fructose-induced deterioration in left ventricular–arterial coupling in Wistar rats. *Br J Pharmacol* 2007;151(3):341–6.
- [14] Xu KY, Zweier JL, Becker LC. Functional coupling between glycolysis and sarcoplasmic reticulum Ca^{2+} transport. *Circ Res* 1995;77(1):88–97.
- [15] Mayes PA. Intermediary metabolism of fructose. *Am J Clin Nutr* 1993;58(5 Suppl):754S–65S.
- [16] Pretorius L, Owen KL, McMullen JR. Role of phosphoinositide 3-kinases in regulating cardiac function. *Front Biosci* 2009;14:2221–9.
- [17] Hyakukoku M, Higashiura K, Ura N, Murakami H, Yamaguchi K, Wang L, et al. Tissue-specific impairment of insulin signaling in vasculature and skeletal muscle of fructose-fed rats. *Hypertens Res* 2003;26(2):169–76.
- [18] Zhu H, Tannous P, Johnstone JL, Kong Y, Shelton JM, Richardson JA, et al. Cardiac autophagy is a maladaptive response to hemodynamic stress. *J Clin Invest* 2007;117(7):1782–93.
- [19] Dorn II GW. Apoptotic and non-apoptotic programmed cardiomyocyte death in ventricular remodeling. *Cardiovasc Res* 2009;81(3):465–73.
- [20] Scherz-Shouval R, Elazar Z. Regulation of autophagy by ROS: physiology and pathology. *Trends Biochem Sci* 2010;36(1):30–8.
- [21] Gustafsson AB, Gottlieb RA. Autophagy in ischemic heart disease. *Circ Res* 2009;104(2):150–8.
- [22] Mellor K, Ritchie RH, Meredith G, Woodman OL, Morris MJ, Delbridge LM. High-fructose diet elevates myocardial superoxide generation in mice in the absence of cardiac hypertrophy. *Nutrition* 2009;26:842–8.
- [23] Jung CH, Ro SH, Cao J, Otto NM, Kim DH. mTOR regulation of autophagy. *FEBS Lett* 2010;584(7):1287–95.
- [24] Reeves PG, Rossow KL, Lindlauf J. Development and testing of the AIN-93 purified diets for rodents: results on growth, kidney calcification and bone mineralization in rats and mice. *J Nutr* 1993;123(11):1923–31.
- [25] Whitesall SE, Hoff JB, Vollmer AP, D'Alecy LG. Comparison of simultaneous measurement of mouse systolic arterial blood pressure by radiotelemetry and tail-cuff methods. *Am J Physiol Heart Circ Physiol* 2004;286(6):H2408–15.
- [26] Peterson GL. A simplification of the protein assay method of Lowry et al. which is more generally applicable. *Anal Biochem* 1977;83(2):346–56.
- [27] Livak KJ, Schmittgen TD. Analysis of relative gene expression data using real-time quantitative PCR and the 2^{(-Delta Delta C(T))} Method. *Methods* 2001;25(4):402–8.
- [28] Howlett SE, Grandy SA, Ferrier GR. Calcium spark properties in ventricular myocytes are altered in aged mice. *Am J Physiol Heart Circ Physiol* 2006;290(4):H1566–74.
- [29] Satoh H, Delbridge LM, Blatter LA, Bers DM. Surface:volume relationship in cardiac myocytes studied with confocal microscopy and membrane capacitance measurements: species-dependence and developmental effects. *Biophys J* 1996;70(3):1494–504.
- [30] Curl CL, Bellair CJ, Harris PJ, Allman BE, Roberts A, Nugent KA, et al. Single cell volume measurement by quantitative phase microscopy (QPM): a case study of erythrocyte morphology. *Cell Physiol Biochem* 2006;17(5–6):193–200.
- [31] Rickart AJ, Morgan J, Tesch G, Funder JW, Fuller PJ, Young MJ. Deletion of mineralocorticoid receptors from macrophages protects against deoxycorticosterone/salt-induced cardiac fibrosis and increased blood pressure. *Hypertension* 2009;54(3):537–43.
- [32] Ritchie RH, Kiriazis H, Xu Q, Du XJ, Kaye DM. Atrial natriuretic peptide (ANP) prevents diabetic cardiomyopathy via suppression of NADPH oxidase. *Circulation* 2006;114(18 Supplement 5):132.
- [33] Rajasekar P, Anuradha CV. Fructose-induced hepatic gluconeogenesis: effect of L-carnitine. *Life Sci* 2007;80(13):1176–83.
- [34] Delbosc S, Paizanis E, Magous R, Araiz C, Dima T, Cristol JP, et al. Involvement of oxidative stress and NADPH oxidase activation in the development of cardiovascular complications in a model of insulin resistance, the fructose-fed rat. *Atherosclerosis* 2005;179(1):43–9.
- [35] Xing SS, Tan HW, Bi XP, Zhong M, Zhang Y, Zhang W. Felodipine reduces cardiac expression of IL-18 and perivascular fibrosis in fructose-fed rats. *Mol Med* 2008;14(7–8):395–402.
- [36] Renna NF, Vazquez MA, Lama MC, Gonzalez ES, Miatello RM. Effect of chronic aspirin administration on an experimental model of metabolic syndrome. *Clin Exp Pharmacol Physiol* 2009;36(2):162–8.
- [37] Mellor KM, Ritchie RH, Davidoff AJ, Delbridge LMD. Elevated dietary sugar and the heart: experimental models and myocardial remodeling. *Can J Physiol Pharmacol* 2010;88(5):525–40.
- [38] Farah V, Elased KM, Chen Y, Key MP, Cunha TS, Irigoyen MC, et al. Nocturnal hypertension in mice consuming a high fructose diet. *Auton Neurosci* 2006;130(1–2):41–50.
- [39] Krook A, Roth RA, Jiang XJ, Zierath JR, Wallberg-Henriksson H. Insulin-stimulated Akt kinase activity is reduced in skeletal muscle from NIDDM subjects. *Diabetes* 1998;47(8):1281–6.
- [40] Briat A, Slimani L, Perret P, Villemain D, Halimi S, Demongeot J, et al. In vivo assessment of cardiac insulin resistance by nuclear probes using an iodinated tracer of glucose transport. *Eur J Nucl Med Mol Imaging* 2007;34(11):1756–64.
- [41] Huggins CE, Domenighetti AA, Ritchie ME, Khalil N, Favalaro JM, Proietto J, et al. Functional and metabolic remodelling in GLUT4-deficient hearts confers hyper-responsiveness to substrate intervention. *J Mol Cell Cardiol* 2008;44(2):270–80.
- [42] Kaczmarczyk SJ, Andrikopoulos S, Favalaro J, Domenighetti AA, Dunn A, Ernst M, et al. Threshold effects of glucose transporter-4 (GLUT4) deficiency on cardiac glucose uptake and development of hypertrophy. *J Mol Endocrinol* 2003;31(3):449–59.
- [43] Huang JP, Huang SS, Deng JY, Hung LM. Impairment of insulin-stimulated Akt/GLUT4 signaling is associated with cardiac contractile dysfunction and aggravates I/R injury in STZ-diabetic rats. *J Biomed Sci* 2009;16:77.

- [44] Dong F, Ren J. Adiponectin improves cardiomyocyte contractile function in db/db diabetic obese mice. *Obesity* (Silver Spring) 2009;17(2):262–8.
- [45] Huisamen B. Protein kinase B in the diabetic heart. *Mol Cell Biochem* 2003;249(1–2):31–8.
- [46] Mizushima N, Yamamoto A, Matsui M, Yoshimori T, Ohsumi Y. In vivo analysis of autophagy in response to nutrient starvation using transgenic mice expressing a fluorescent autophagosome marker. *Mol Biol Cell* 2004;15(3):1101–11.
- [47] Martinet W, Knaapen MW, Kockx MM, De Meyer GR. Autophagy in cardiovascular disease. *Trends Mol Med* 2007;13(11):482–91.
- [48] Kuma A, Hatano M, Matsui M, Yamamoto A, Nakaya H, Yoshimori T, et al. The role of autophagy during the early neonatal starvation period. *Nature* 2004;432(7020):1032–6.
- [49] Dikalov S, Griendling KK, Harrison DG. Measurement of reactive oxygen species in cardiovascular studies. *Hypertension* 2007;49(4):717–27.
- [50] Qin B, Polansky MM, Harry D, Anderson RA. Green tea polyphenols improve cardiac muscle mRNA and protein levels of signal pathways related to insulin and lipid metabolism and inflammation in insulin-resistant rats. *Mol Nutr Food Res* 2010;54(Suppl 1):S14–23.
- [51] Domenighetti AA, Danes VR, Curl CL, Favalaro JM, Proietto J, Delbridge LM. Targeted GLUT-4 deficiency in the heart induces cardiomyocyte hypertrophy and impaired contractility linked with Ca(2+) and proton flux dysregulation. *J Mol Cell Cardiol* 2010;48(4):663–72.
- [52] Barone S, Fussell SL, Singh AK, Lucas F, Xu J, Kim C, et al. Slc2a5 (Glut5) is essential for the absorption of fructose in the intestine and generation of fructose-induced hypertension. *J Biol Chem* 2009;284(8):5056–66.
- [53] Levi B, Werman MJ. Long-term fructose consumption accelerates glycation and several age-related variables in male rats. *J Nutr* 1998;128(9):1442–9.
- [54] Havel PJ. Dietary fructose: implications for dysregulation of energy homeostasis and lipid/carbohydrate metabolism. *Nutr Rev* 2005;63(5):133–57.
- [55] Cao J, Xu D, Wang D, Wu R, Zhang L, Zhu H, et al. ROS-driven Akt dephosphorylation at Ser-473 is involved in 4-HPR-mediated apoptosis in NB4 cells. *Free Radic Biol Med* 2009;47(5):536–47.
- [56] Yuan H, Perry CN, Huang C, Iwai-Kanai E, Carreira RS, Glembofski CC, et al. LPS-induced autophagy is mediated by oxidative signaling in cardiomyocytes and is associated with cytoprotection. *Am J Physiol Heart Circ Physiol* 2009;296(2):H470–9.
- [57] Younce CW, Wang K, Kolattukudy PE. Hyperglycemia-induced cardiomyocyte death is mediated via MCP-1 production and induction of a novel zinc-finger protein MCP1P. *Cardiovasc Res* 2010;87(4):665–74.
- [58] Mammucari C, Schiaffino S, Sandri M. Downstream of Akt: FoxO3 and mTOR in the regulation of autophagy in skeletal muscle. *Autophagy* 2008;4(4):524–6.
- [59] Chang NC, Nguyen M, Germain M, Shore GC. Antagonism of Beclin 1-dependent autophagy by BCL-2 at the endoplasmic reticulum requires NAF-1. *EMBO J* 2010;29(3):606–18.
- [60] Giani JF, Munoz MC, Mayer MA, Veiras LC, Arranz C, Taira CA, et al. Angiotensin-(1–7) improves cardiac remodeling and inhibits growth-promoting pathways in heart of fructose-fed rats. *Am J Physiol Heart Circ Physiol* 2010;298(3):H1003–13.
- [61] Kamide K, Rakugi H, Higaki J, Okamura A, Nagai M, Moriguchi K, et al. The renin-angiotensin and adrenergic nervous system in cardiac hypertrophy in fructose-fed rats. *Am J Hypertens* 2002;15(1 Pt 1):66–71.